Structure and dynamics in colloidal and porous charged media

2002 J. Phys.: Condens. Matter 14 9207

(http://iopscience.iop.org/0953-8984/14/40/312)

INSTITUTE OF PHYSICS PUBLISHING JOURNAL OF PHYSICS: CONDENSED MATTER

J. Phys.: Condens. Matter **14** (2002) 9207–9221 PII: S0953-8984(02)36550-0

Structure and dynamics in colloidal and porous charged media

V Marry[1], F Grün[2], C Simon[1], M Jardat[1], P Turq[1] and C Amatore[2]

[1] Laboratoire Liquides Ioniques et Interfaces Chargées, Case 51, Université P et M Curie, 4 place Jussieu, F-75252 Paris Cedex 05, France
[2] UMR Pasteur, Ecole Normale Supérieure, 24 rue Lhomond, F-75005 Paris, France

Received 2 May 2002, in final form 26 June 2002
Published 27 September 2002
Online at stacks.iop.org/JPhysCM/14/9207

Abstract

Two examples of charged media in water are studied by numerical simulations: aqueous solutions of highly asymmetrical electrolytes (large and highly charged spherical particles surrounded by small and slightly charged counterions) and a swelling clay (charged plane sheets surrounded by small counterions). In the former example, Brownian dynamics (BD) showed that the mean number of counterions in the vicinity of polyions nearly balances the charge of the macroion and that the turnover of the small ions in this region is important. The effect of hydrodynamic interactions on the dynamics is weak for small ions but is great for macroions. On the other hand, the relative decrease of the macroion self-diffusion coefficients is more important than that of counterions. Moreover, the small ions retain a relatively high self-diffusion coefficient at the highest concentration, a concentration at which the macroions freeze. BD simulation was also used to obtain the distribution of counterions Na^+ between the sheets of a fairly hydrated montmorillonite. The obtained profile was very similar to those we obtained by atomic simulations (Monte Carlo and molecular dynamics) and by a Poisson–Boltzmann treatment. It justifies the description of the solvent as a continuum as soon as the system is hydrated enough. However, for less hydrated states of the clay (mono- or bi-layer of water), only atomic simulations can bring exploitable information. We showed that, according to whether the counterion is Na^+ and/or Cs^+, the behaviours in the bihydrated clay are very different: although Na^+ is easily hydrated and is located in the middle of the pores, Cs^+ remains close to the negative surfaces of the sheets and its preferential paths along the surface sites can be underscored from obtained trajectories.

1. Introduction

The structural and dynamical properties of charged colloidal suspensions and charged porous media may be investigated at different levels of description [1, 2]: at the microscopic one

solvent molecules are considered explicitly, whereas the solvent is treated as a dielectric continuum at the mesoscopic level of description. In both cases the common ingredients for the modelling of the system are Coulomb interactions and the excluded volume effects. The microscopic dynamics is relevant for direct numerical molecular dynamics, and the mesoscopic dynamics can be studied either from numerical Brownian dynamics (BD) or from hydrodynamical analytical models. Colloidal suspensions and porous media are here considered together because, from a geometrical point of view, porous media appear as a complementary image of concentrated colloidal suspensions, the void parts in the porous medium corresponding to the solute colloidal part in the suspension. The strong Coulomb interactions give general features to these systems, such as counterions condensation, electrokinetic flows (zeta potential) or long-range screening conditions, which provide the unity of this subject. The case of clays is typical of this unity since, according to the clay/water ratio, one goes from compact systems with small pores containing few layers of water molecules to suspensions exhibiting full charged colloidal features.

The microscopic models, in which both solvent molecules and solid species are considered explicitly as molecular entities, are surely the most satisfying models of the latter systems. In any case, the model dependence of discrete simulations remains an open question. Polarizability and polarization effects on ions and water molecules have surely to be considered in order to improve the description of aqueous systems; they however increase the heaviness of calculations in a non-tractable way. Quantum simulations (such as Car–Parrinello molecular dynamics [3]) in fact rarely lead to simulation times longer than 100 ps. The number of particles then limits the applicability of discrete solvent simulations to the case of non-polarizable molecules. Practically, only porous media and solutions of very small molecules were treated on this level of description.

Analytical dynamical models are traditional in the field of charged colloids and charged porous media [4, 5]. They are particularly suitable to include proper links with hydrodynamics and they are also connected to the short-ranged dynamics by the use of mode coupling theories. Such calculations are usually restricted to DLVO-like models for colloidal suspensions and Smoluchowski-like models for porous media. Nevertheless, the one-component models of colloidal suspensions, which neglect the finite size of small counterions and coions and the interactions between them, may be inadequate in the detailed description of polyion systems at finite concentration [6, 7]. Theoretical calculations and computer simulations based on the primitive model, which consider explicitly all solute particles as charged hard spheres, have shown that the influence of counterions on the structural properties of colloidal suspensions may be striking [8–11].

Here, we present two examples of colloidal and porous charged media studied at several levels of description. Firstly, structural and dynamical properties of aqueous solutions of highly asymmetrical electrolytes are investigated, at the mesoscopic level, from BD simulation. In that case, both counterions and polyions are explicitly considered in the framework of the continuous solvent model. Next, a swelling clay is studied at both the microscopic and the mesoscopic levels. The latter example allows us to outline the significance of each model.

The present paper is organized as follows. In section 2, we report the results obtained from BD simulations without hydrodynamic interactions (HIs), concerning 1–10, 1–20 and 2–20 aqueous electrolytes [12]. We also present new results concerning the dynamics of ions in these systems, obtained by BD including HI. We then address the problem of structural and dynamical properties of ions inserted in an hydrated montmorillonite (section 3), which is an example of a charged porous medium. In the latter case several approaches to the same problem will be compared: molecular dynamics simulation, BD simulation and analytical calculations.

2. Structural and dynamical properties of highly asymmetrical electrolyte solution on the mesocopic scale

Several articles have recently been published concerning the structural properties of highly asymmetrical electrolytes in solution, with charge asymmetry of 1–20, 2–20 [13–17] or 1–60 to 3–60 [18–21], the 1–20 and 1–60 representing aqueous micellar solutions of sodium *n*-octylsulfate and sodium *n*-dodecylsulfate. All these studies of highly asymmetrical electrolytes based on two-component models concern the structural and thermodynamical properties of the solutions. Their dynamical properties have been investigated with the help of the BD simulation, which describes the suspension on a mesoscopic scale [12]. Aqueous solutions of 1–10, 1–20 and 2–20 electrolytes with an asymmetry in size of 2:15 were simulated for four macroion densities between 3×10^{-6} and 30×10^{-6} Å^{-3}, which correspond to concentrations between 0.005 and 0.05 mol l^{-1}. The different length and timescales of macroions and counterions in such systems make the simulation of their properties rather tricky. An efficient BD simulation [22] method was used, which allows us to choose large time steps and to generate long trajectories for the particles. The pair interaction potential between ions was modelled by a pairwise soft-core repulsion ($1/r^9$) and the Coulomb interaction, whose long range is taken into account thanks to an Ewald summation [23]. Here we investigate the effect of HI on ion dynamics. To our knowledge, this is the first simulation including HI of a two-component model for a highly asymmetrical electrolyte in solution. First we briefly recall the principles of the BD (section 2.1), and then we present the structural (section 2.2.1) and dynamical (section 2.2.2) results.

2.1. The Brownian dynamics simulation

On the mesoscopic timescale of BD, the solvent is treated as a dielectric continuum of viscosity η (usually that of the pure solvent). The velocities of the solute are supposed to be in equilibrium with the solvent part so that the motions of particles are described in the position space only. The numerical simulation on this level is based on a stochastic equation of motion for the displacement $\Delta \boldsymbol{r}$ from t to $t + \Delta t$ of the N particles [24]

$$\Delta \boldsymbol{r} = \left(\beta \boldsymbol{D} \cdot \boldsymbol{F} + \frac{\partial}{\partial \boldsymbol{r}} \cdot \boldsymbol{D} \right) \Delta t + \boldsymbol{R}, \tag{1}$$

where $\beta = 1/k_{\mathrm{B}}T$. Here, the particles are supposed to be spherical, without rotational degree of freedom; Δt is the time increment, $\boldsymbol{r} = (\boldsymbol{r}_1^T, \boldsymbol{r}_2^T, \ldots, \boldsymbol{r}_N^T)^T$ is the $3N$-dimensional configuration vector and $\boldsymbol{F} = (\boldsymbol{F}_1^T, \ldots, \boldsymbol{F}_N^T)^T$ describes the forces acting on the particles at the beginning of the step. $\boldsymbol{R}$ is a random displacement, chosen from a Gaussian distribution with zero mean, $\langle \boldsymbol{R} \rangle = 0$ and variance $\langle \boldsymbol{R}\boldsymbol{R}^T \rangle = 2\boldsymbol{D}\Delta t$. HI between particles can be introduced via the configuration-dependent $3N \times 3N$ diffusion tensor $\boldsymbol{D}$. If they are neglected, the matrix $\boldsymbol{D}$ is diagonal and constant, with eigenvalues equal to the self-diffusion coefficients of ions at infinite dilution, referred to as D_i^0 for ion i. Each displacement obtained from equation (1) is accepted according to the smart Monte Carlo acceptance criterion [22, 25].

Two sets of simulations were performed. The first one [12] concerns 1–10, 1–20 and 2–20 electrolyte solutions at four concentrations: 0.004 89, 0.01, 0.02 and 0.05 mol l^{-1}. In each case, 80 macroions and the corresponding number of counterions were placed in a cubic box with periodic boundary conditions. Due to the large number of particles, HI are neglected in this case. The second one concerns the 2–20 electrolyte at 0.01 and 0.02 mol l^{-1}: only 30 macroions are considered, which allowed us to take into account HI between all solute particles. In any case, the parameters of the interaction potential were those given in [12]. To compute the soft-core interactions we used a spherical cut-off of half a box

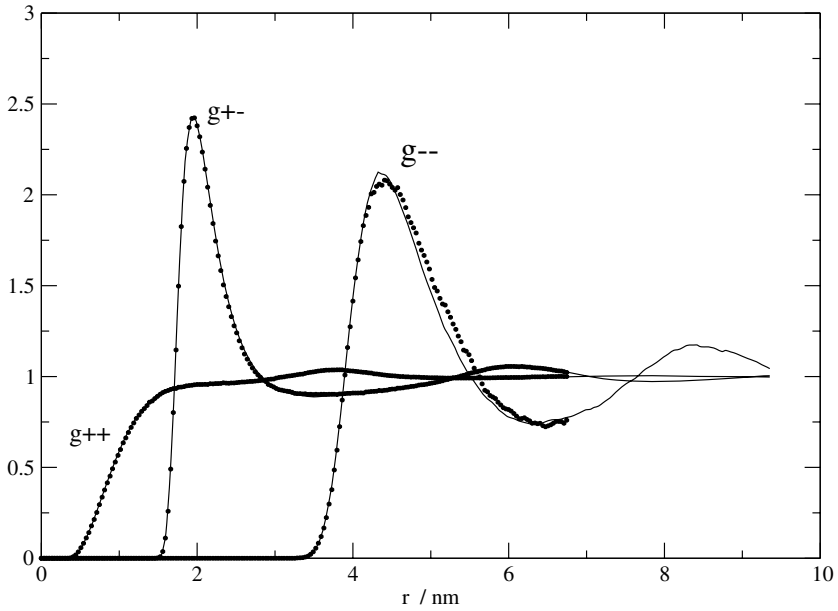

Figure 1. RDFs for the 2–20 aqueous solutions at 0.02 mol l^{-1} at 298 K obtained using BD simulation (solid curve, 80 polyions in the simulation box; filled circles, 30 polyions in the simulation box).

length, applying the minimum image convention. Coulomb interactions were computed by using the Ewald summation technique [23, 26] with the conducting boundary condition. The diffusion matrix was modelled by the Rotne–Prager tensor [27], which is calculated with the same approximations as in [22]. The self-diffusion coefficients at infinite dilution are $D^0_{ion} = 1.3\times10^{-9}\,m^2\,s^{-1}$ and $D^0_{macroion} = 0.16\times10^{-9}\,m^2\,s^{-1}$. The former is the experimental value corresponding to the sodium ion and the latter is related to the radius $a_{macroion}$ of the macroion through the Stokes formula.

Structural and dynamical properties were calculated by averaging over five successive trajectories, whose duration was about 15 ns, while the equilibration runs lasted for about 100 ns time frames.

The self-diffusion coefficients of both counterion and macroion were calculated in each solution by the mean square displacements:

$$D_i = \lim_{t\to\infty} \frac{\langle (\boldsymbol{r}_i(t) - \boldsymbol{r}_i(0))^2 \rangle}{6t}. \tag{2}$$

We also computed the residence time of counterions in the vicinity of macroions, following Impey *et al* [28]. In this calculation, the characteristic distance under which the small ions are supposed to be condensed on polyions was that at which the macroion–counterion radial distribution function (RDF) has its first minimum.

2.2. Results

2.2.1. Structural properties. We checked that simulations without and with HI led to the same pair correlation functions. Moreover, as shown in figure 1, both simulations of the 2–20 electrolyte solution at 0.02 mol l^{-1} (either with 80 or with 30 polyions in the cubic box) lead to the same RDFs.

Table 1. Average number of counterions condensed on the macroions at distances lower than the minimum of the macroion–counterion RDF at 298 K.

	0.004 98 mol l^{-1}	0.01 mol l^{-1}	0.02 mol l^{-1}	0.05 mol l^{-1}
1–20[a]	14	15	23	50
2–20[a]	7.5	7	9	22
2–20[b]		7	9	

[a] From [12]: BD simulations with 80 macroions in the cubic box.
[b] BD simulations with 30 macroions in the cubic box.

Table 2. Residence times (ps) of the counterions in the vicinity of macroions obtained from BD simulations of aqueous solutions of 1–20 and 2–20 electrolytes at 298 K.

	0.00498 mol l^{-1}	0.01 mol l^{-1}	0.02 mol l^{-1}	0.05 mol l^{-1}
1–20[a]	2950	1750	1550	1750
2–20[a]	4610	2260	1760	2030
2–20[b]		1520	1110	
2–20[c]		1450	1160	

[a] From [12]: BD simulations without HI, with 80 macroions in the cubic box.
[b] BD simulations without HI, with 30 macroions in the cubic box.
[c] BD simulations with HI, with 30 macroions in the cubic box.

An important result is that, at the highest concentration, the macroion–macroion RDFs reveal a structuring of the system [12]. This freezing is confirmed by the values of macroion self-diffusion coefficients, which become very small at this concentration (see the following section). Indeed, a crystallization of macroions in a face-centred cubic phase occurs for the 1–20 and 2–20 electrolytes. In the 1–10 electrolyte at the same volume fraction, the macroions remain in a disordered structure.

The coordination number of polyions was also calculated [12] (see table 1): it is defined as the average number of counterions present in the vicinity of polyions, the characteristic distance R_c below which a small ion is considered to be condensed on the macroion corresponding in any case to the minimum of the macroion–counterion RDF. The number of condensed ions increases with the concentration and is nearly sufficient to neutralize the macroions at 0.02 mol l^{-1}. It can be noticed that simulations of the 2–20 electrolyte at 0.01 and 0.02 mol l^{-1}, with 30 or 80 polyions in the simulation box, lead to the same result. At the highest concentration, the coordination number exceeds the value sufficient to neutralize the macroion, which is due to the closeness of macroions.

2.2.2. Dynamical properties. The residence times of the small ions in the vicinity of polyions were calculated; results are given in table 2. For the three lower concentrations, the residence time decreases as the concentration increases. At a given macroion density, the residence time is larger for the 2–20 electrolyte than for the 1–20 one, as the electrostatic attraction between ions of opposite charges is all the more intensive as the salt is dilute and as the counterion is charged. On the other hand, the residence time is higher at 0.05 than 0.02 mol l^{-1}: the closeness of macroions in the former solution leads to the sharing of their coordination shells. In any case, the residence time is of the order of the time needed by the counterion to cover a distance $d = R_c - a_{macroion}$ ($a_{macroion}$ being the radius of the macroion), which is about 25 Å ($d^2/D^0_{ion} = 4800$ ps). Simulations with only 30 macroions in the cubic box lead to a residence time of the same order of magnitude as the previous simulations. Finally, we show that HIs have little influence on the residence time.

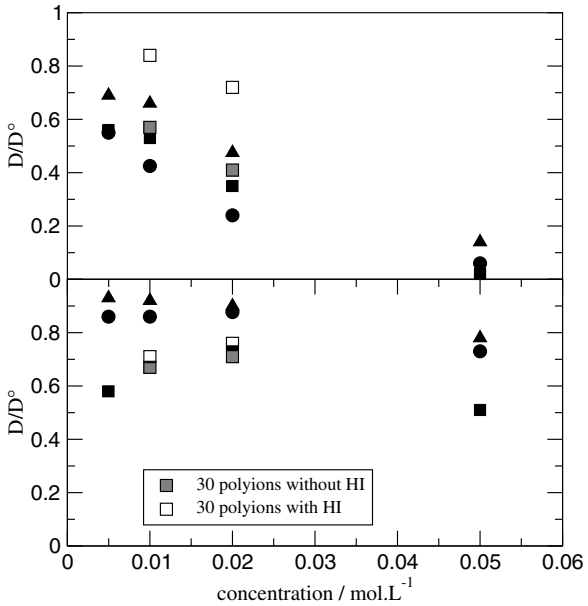

Figure 2. Ratio between the self-diffusion coefficient and the value at infinite dilution for the macroion (upper graph) and for the counterion (the graph below), obtained from BD simulations: 1–20 electrolyte (circles), 2–20 electrolyte (squares) and 1–10 electrolyte (triangles).

The ratios between the self-diffusion coefficients of ions obtained from BD simulations and the values at infinite dilution are given in figure 2. Both simulations without HI of the 2–20 electrolyte at 0.01 and 0.02 mol l^{-1} (with 30 and 80 macroions in the simulation box) lead to self-diffusion coefficients in good agreement. As can be observed in figure 2, the self-diffusion coefficients of small ions vary slightly when the concentration increases, whereas those of the macroions are strongly decreased. At the highest concentration, the macroions crystallize and no longer diffuse, whereas the counterions retain a relatively high self-diffusion coefficient. On the other hand, the influence of HI on the self-diffusion is great for macroions of the 2–20 electrolyte at 0.01 and 0.02 mol l^{-1}, whereas HI seem to have little influence on the self-diffusion of counterions. This effect of HI on the dynamics of colloidal particles has already been observed experimentally [29] and also by a mode-coupling theory for colloids [30].

2.2.3. Conclusion. The BD simulation allowed us to investigate the dynamical properties of highly asymmetrical electrolyte in aqueous solution. It was shown that the mean number of counterions in the vicinity of polyions nearly balances the charge of the macroion at the three lowest concentrations and that the turnover of the small ions in this region is important. The effect of HI on the dynamics is weak for the small ions but seems to be great for the macroions. On the other hand, the relative decrease of the macroion self-diffusion coefficients is more important than that of counterions. Moreover, the small ions retain a relatively high self-diffusion coefficient at the highest concentration, a concentration at which the macroions freeze. The latter situation may be related to that of ions moving between charged planes, as is the case in swelling clays.

3. Multiscale study of structural and dynamical properties of ions in a swelling clay

Because of their low permeability and their retention properties, compacted clays present a great interest for nuclear waste storage. Thus, their large specific surface when dispersed confers catalyst behaviour on them.

Swelling clays have a quite interesting behaviour towards water. According to their degree of hydration, their aspect goes from the powder to the aqueous suspension, through the gel. They are made of large particles (around 1000 Å long), constituted by a stacking of negatively charged layers of aluminosilicate. The negative charge is compensated by counterions, often Na^+ and Ca^{2+} in natural soils, located between sheets and on particle surfaces. When a dry clay is in contact with water, the former adsorbs on surfaces and between the sheets, leading to an increasing of the interlayer spacing of the particles. This crystalline swelling is partly explained by the hydration capacity of counterions and accordingly leads to the step by step formation of a mono-, a bi- or a tri-layer of water. When the hydration is further increased, the water adsorbs in meso- and macro-pores and the swelling due to sheets withdrawing becomes continuous: this is osmotic swelling. According to the degree of hydration of the clay, several descriptions and models are available and comparisons between them are possible [31–34]. In this article, we shall concentrate on different suggested models to describe the interlayer spacing of a montmorillonite. It will be shown that the atomic description of the system used in microscopic simulations has a non-negligible influence on water and cation structure and dynamics, especially for less hydrated states. However, a comparison between microscopic simulations on more hydrated states and other methods such as continuous solvent simulations and analytical Poisson–Boltzmann treatment show that simpler descriptions of the system can be enough to give certain information on the hydrated clay.

3.1. Atomic description. Microscopic simulations

Microscopic simulations based on Monte Carlo and molecular dynamics methods allow us to describe less hydrated states of the clay [35, 35–46], at least on the sheet scale. On this level of description, clay sheets and water molecules are described as discrete ensembles of atoms. The simulations well reproduce variations in interlayer spacings with the degree of hydration and step-by-step swelling behaviours [35–37, 40, 41, 44, 46]. They allow a precise description of the structure and the dynamics of ions and water molecules in the interlayer spacing, according to the configuration and the preferential sites of clay sheets [39–41, 44, 46]. As an example, we present first new results obtained on a bihydrated Na montmorillonite (i.e. containing two layers of water), in which Cs^+ has been introduced. This configuration can give an idea of the behaviour of a radionuclide Cs^+ in a natural compacted montmorillonite whose counterion is Na^+. Indeed, interlayer spacings constitute the major part of the porosity in bentonites of dry densities $> 1.8\ \mathrm{kg\,l^{-1}}$ [47]. For a dry density of $2\ \mathrm{kg\,l^{-1}}$, the pore size has been evaluated at 6.6 Å, which corresponds to the bihydrated state [48]. It is likely that traces of caesium can diffuse in this kind of space neutralized by natural counterions such as Na^+.

3.1.1. Simulation method. According to the case, the box simulation contains one or two clay sheets, i.e. one or two interlayer spaces, in which are introduced water molecules and counterions. For less hydrated states where the value of the interlayer spacing is too low, two sheets are necessary in order to allow the vertical dimension of the box to be higher than twice the minimal cut-off distance for interaction calculation (i.e. 2×7.9 Å). The simulation box is given in figure 3. For well hydrated states, the box with a sole sheet is enough. Positions of atoms in the sheets are deduced from x-ray diffraction measurements [49, 50]. The formula

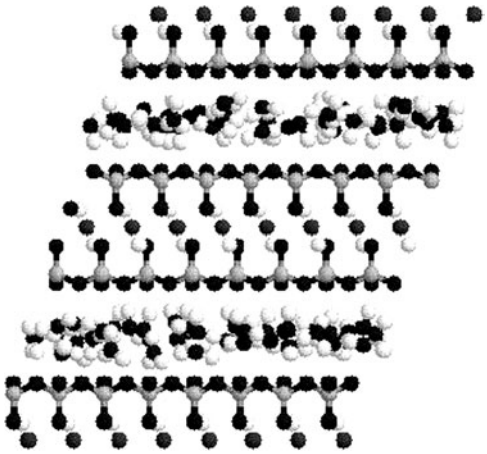

Figure 3. A simulation box constituted by two clay sheets.

of the chosen montmorillonite is $C_{0.75}[Si_8](Al_{3.25}Mg_{0.75})O_{20}(OH)_4$. Each sheet contains eight unit cells, its dimensions are 20.72×17.94 Å^2 and its thickness is 6.44 Å. Each interlayer spacing contains six counterions. Sheets and water molecules are rigid. The model chosen for water is the SPC/E model. The interactions between atoms are divided into electrostatic and van der Waals contributions, given by a Lennard-Jones potential. Clay parameters for Lennard-Jones potentials are Smith's ones [44].

Monte Carlo simulations in the (N, P, T) ensemble were used to equilibrate the system. Clay sheets were allowed to move vertically, as well as horizontally. According to the number of water molecules and the chosen pressure and temperature ($P = 1$ bar and $T = 298$ K), the value of the equilibrated interlayer spacing and the favourable positions of the sheets can be obtained. Transport properties can then be evaluated by molecular dynamics in the (N, V, T) ensemble, where sheets are motionless.

3.1.2. Results on a bihydrated montmorillonite. The bihydrated Na montmorillonite is well described when the simulation box contains 72 water molecules per interlayer spacing. The corresponding value of the equilibrated interlayer spacing (i.e. the distance between the middle of two clay sheets) is 15.2 Å. We started from this configuration to simulate a similar system where one Na^+ is replaced by one Cs^+ in each interlayer space.

The obtained distributions as a function of the vertical position z for Na^+, Cs^+ and water oxygens are given in figure 4.

The two peaks on the oxygen distribution effectively reveal the presence of two layers of water in the interlayer space. The profiles for Na^+ and Cs^+ are quite different since two peaks are present in the Cs distribution and only one peak in the Na distribution. The same profiles were obtained in the same montmorillonite containing only Na^+ and only Cs^+ [42, 46]. This is due to the fact that Na^+ are much more hydrated than Cs^+, which rather have strong interactions with the surface oxygens of the sheets. In the bihydrated clay, Na^+ is surrounded by six water molecules, as in bulk water, although Cs^+ has a coordination number of 8.2, which is lower than in bulk water (9.2 in an aqueous solution of two CsCl per 281 H_2O with the same potentials of interaction). This explains why experimentally the crystalline swelling of Na montmorillonites can reach the trilayer, although Cs montmorillonites remain in a monohydrated state, where Cs^+ maintain a cohesion between the opposite sheet surfaces of the interlayer space.

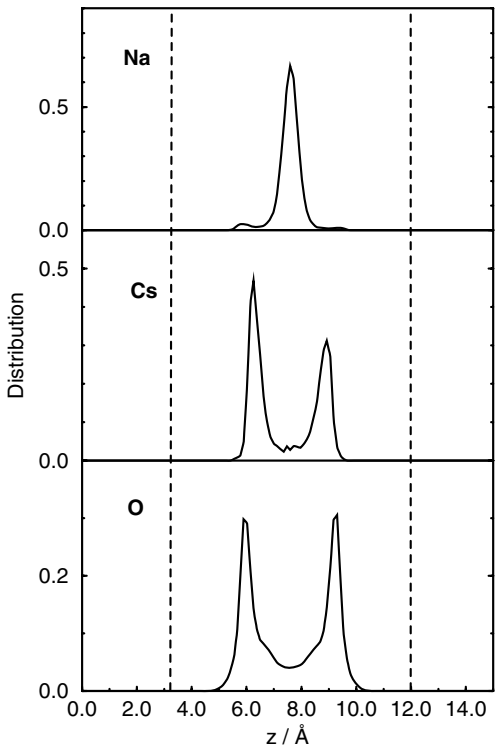

Figure 4. Normalized distributions of water oxygens and counterions Na^+ and Cs^+, as a function of their vertical position z. The dashed lines represent the surfaces of the sheets.

From molecular dynamics, cations' trajectories can be obtained to underscore the eventual existence of preferential sites on sheet surfaces. A horizontal 640 ps trajectory of a Cs^+ is given in figure 5. As, in contrast to Na^+, Cs^+ has a tendency to remain close to the surfaces, it was easier to enhance sites of preferential interactions of this cation with them. The cation moves from one surface to another but slowly enough to be able to underscore a path along one of the surfaces. Then, the interlayer space was cut in two parts and on the figure is only given the part of the trajectory where the cation is closer to one of the surfaces. Oxygen and silicon atoms of this surface are represented on the figure. Cs^+ in a bihydrated Na montmorillonite seems to go preferentially on sites constituted by silicon atoms surrounded by three oxygens. Even in the presence of structuring cations such as Na^+, the behaviour of Cs^+ is very similar to that found in simulations on homoionic Cs-clays [44, 46].

Diffusion coefficients are calculated thanks to the two-dimensional Einstein relation:

$$D = \lim_{t\to\infty} \frac{\langle \boldsymbol{r}(t) - \boldsymbol{r}(0)^2 \rangle}{4t} \tag{3}$$

where $\boldsymbol{r}(t)$ is the particle position at t.

Let us notice that the two-dimensional relation was chosen since the mean-square displacement along z is bounded. Indeed, the simulation time used to compute the diffusion coefficients is larger than the time needed to cross the interlayer distance.

Diffusion coefficients for water molecules, Na^+ and Cs^+ are respectively 1.8×10^{-9}, 9.6×10^{-10} and 1.2×10^{-9} m^2 s^{-1}. These values are several times higher than the calculated diffusion coefficients in the monohydrated state [46] (2.6×10^{-10}, 8.2×10^{-11}

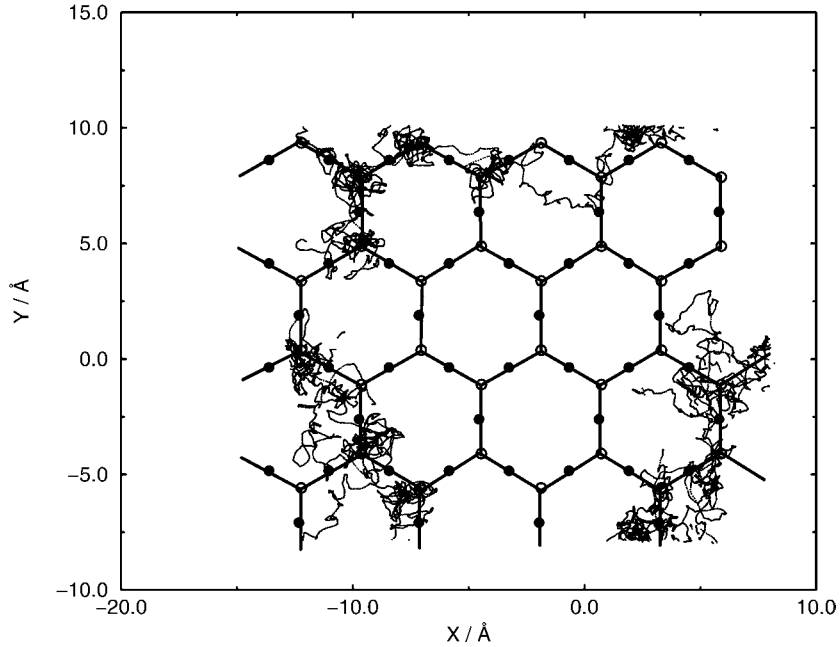

Figure 5. Horizontal trajectory of a Cs^+ in the bihydrated Na montmorillonite, close to one of the sheet surfaces: filled circles, oxygen surface atoms; open circles, silicon surface atoms. Solid lines link silicon atoms of the surface.

and 1.9×10^{-10} m^2 s^{-1} respectively), but they are lower then those in bulk water (2.3×10^{-9}, 1.35×10^{-9} and 2.11×10^{-9} m^2 s^{-1}). As in the monohydrated state, Cs^+ move faster than Na^+ but the difference is less significant.

It is clear that, at this level of description, microscopic simulations bring information that too simple models are not able to reveal, especially concerning water molecule properties (distributions, orientations, way of hydrating cations). Thus, for this low hydration state, only a discrete modellization of the solvent can explain the water layer structure of the interlayer spacing. However, this kind of detailed modelling is time consuming and becomes long and difficult for more hydrated systems. Thus, the more hydrated the clay is, the less significant the influence of the atomic structure of surfaces and solvent will be [51]. Mesoscopic approaches can then be useful to generalize behaviours in more hydrated clays.

3.2. Mesoscopic descriptions

Poisson–Boltzmann remains the simplest analytical model to calculate ion distribution between two charged planes. This is why Poisson–Boltzmann and electrical double-layer theories are often used in the literature to simply describe ion distributions between particles' surfaces in clays [31, 48, 52, 53]. In these models, the sheets are considered as uniformly charged planes. For more detailed descriptions of the system and especially concerning its dynamics, intermediate models based on continuous solvent simulations can be useful. They allow us to work with larger simulation boxes than atomic simulations, and so to obtain better statistics on the results in a smaller simulation time, which is often a problem with microscopic simulations. In this section we make a link between all these methods by comparing the ion distributions we obtained by Poisson–Boltzmann, microscopic and continuous solvent simulations. We

have already shown that Poisson–Boltzmann and microscopic ones were very similar for a box simulation containing 300 water molecules per interlayer space [31], for another type of montmorillonite. We give here new comparisons of profiles between Poisson–Boltzmann and the two methods of simulation. The chosen clay is the same as in the previous section. The hydrated state is represented, in the microscopic description, by a simulation box containing 400 H_2O per interlayer space. The value of the distance between the sheet surfaces after equilibration in the (N, P, T) ensemble is 35.9 Å. This corresponds to a ionic concentration of 0.747 mol l^{-1}. These are the values which are used in the Poisson–Boltzmann treatment and continuous solvent simulations. The counterions are Na^+ only. For significant interlayer spaces and away from the surfaces, the water behaviour is close to the bulk one. The mesoscopic descriptions of this system will then treat the solvent as bulk water (dielectric permittivity $\epsilon_r = 78.3$).

3.2.1. Poisson–Boltzmann treatment. According to Boltzmann statistics, we can express the concentration $c_i(r)$ of the ion i at a distance r from a central particle as

$$c_i(r) = M_i \exp\left(-\frac{V_i(r)}{k_B T}\right) \tag{4}$$

where $V_i(r)$ can be identified with the electrostatic energy $V_i(r) = e_i\psi(r)$. $e_i = Z_i e$ is the charge of i and $\psi(r)$ the electrostatic potential.

Between two uniformly charged planes, ψ and c_i only depend on z. Then, we can write, by integrating $c_i(z)$,

$$\int_{-L/2}^{+L/2} c_i(z)\,\mathrm{d}z = M_i \int_{-L/2}^{+L/2} \exp\left(-\frac{e_i\psi(z)}{k_B T}\right)\mathrm{d}z = L c_i^0 \tag{5}$$

where c_i^0 is the average concentration of i in the interlayer space, and L the distance between the planes.

This equation allows us to calculate M_i. By replacing $\Delta\psi = -\sum_i e_i c_i(r)/\epsilon_0\epsilon_r$ in the Poisson equation, we obtain

$$\Delta\psi = -\sum_i \frac{e_i M_i}{\epsilon_0\epsilon_r} \exp\left(-\frac{e_i\psi}{k_B T}\right). \tag{6}$$

With $\phi = e\psi/k_B T$, this becomes

$$\Delta\phi = -4\pi L_B \sum_i Z_i M_i \mathrm{e}^{-Z_i\phi} \tag{7}$$

where $L_B = e^2/4\pi\epsilon_0\epsilon_r k_B T$ is the Bjerrum length.

Thus, one of the boundary conditions is $\mathrm{d}\phi/\mathrm{d}z\,(z = 0) = 0$, since the system is symmetric.

When the counterions are the only ions in the interlayer space, the differential equation can be analytically solved. The counterionic concentration is then given by

$$c(z) = \frac{1}{2\pi Z^2 L_B} \frac{\alpha^2}{\cos^2(\alpha z)} \tag{8}$$

with $\alpha \tan(\alpha L/2) = 2\pi Z L_B \sigma/e$. σ is the surface charge density.

To allow comparisons with microscopic descriptions, a radius of 2.1 Å was taken for the cation Na^+ and $\sigma = 0.0161/e$ Å^{-2}, which corresponds to the same surface charge density as in the simulation box.

The Poisson–Boltzmann treatment allowed us to obtain the density profile of the counterions between the two charged planes. However, no dynamical property can be easily obtained in this way. We then propose to study the same system from BD simulation.

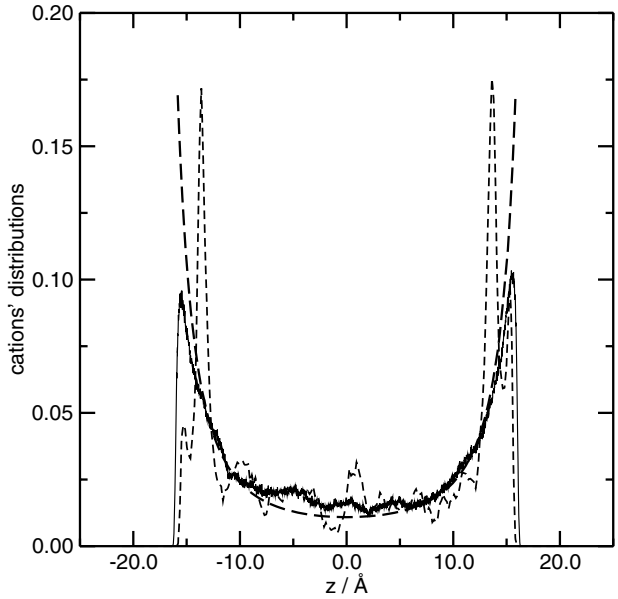

Figure 6. Counterion distributions between the charged planes obtained from molecular dynamics simulation (dashed curve), Poisson–Boltzmann calculation (long-dashed curve) and BD simulation (solid curve).

3.2.2. Brownian dynamics simulation. Here, 60 sodium counterions are placed in a rectangular simulation box, with periodic boundary conditions only in the two directions which are perpendicular to the charge planes. Moreover, the planes carry discrete charged sites, which model the oxygen atoms of the clay. The positions of these sites are the same as in the molecular dynamics simulations. Their charges are chosen in order to obtain the same charge density σ as in the simulation box of section 3.1. Interactions between the counterions and also between counterions and charged sites of the planes are modelled by a short-ranged repulsive contribution ($1/r^{12}$) and a Coulomb part, whose long range is taken into account thanks to a two-dimensional Ewald summation [54, 55]; HIs between ions are neglected in this first study. The radius of counterions is the same as that used in the Poisson–Boltzmann calculation 3.2.1; their self-diffusion coefficient at infinite dilution is that measured in bulk water (1.3×10^{-9} m^2 s^{-1}). Counterions are moved according to the stochastic equation of motion (1) and the displacements are accepted according to the smart Monte Carlo criterion described in section 2. Structural properties were calculated by averaging over nine successive trajectories, whose duration was about 15 ns.

3.2.3. Results. Na^+ distributions are given in figure 6. The three curves represent distributions obtained by microscopic simulation, BD simulation and Poisson–Boltzmann treatment. Their integrals are represented in figure 7. Let us notice the presence of oscillations in both the simulated distributions. They are mainly due to statistical phenomena in the case of BD simulations. On the other hand, the discrete nature of the solvent is another reason for them in the microscopic simulation. It was shown in section 3.1 that the method of counterion hydration near the surface can play a role in cation distributions. The two sharp peaks near the surfaces are located at about 4.3 Å from the surfaces, which is the same as the distance between Na^+ and the surfaces in the bihydrated state of section 3.1. This indicates that, in microscopic

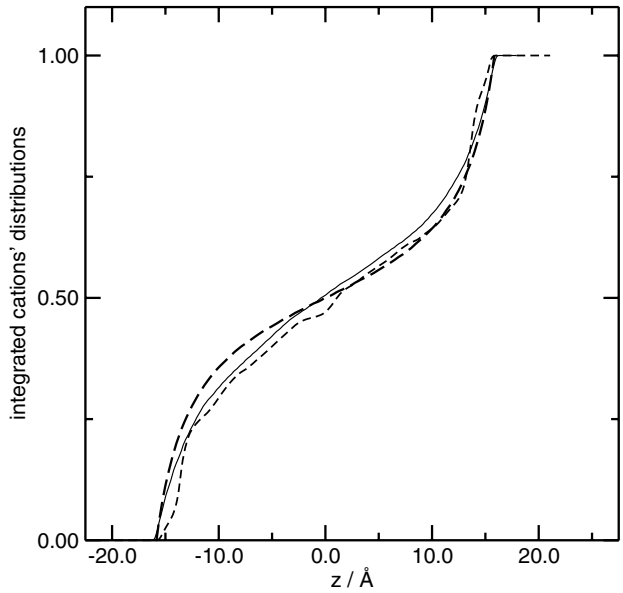

Figure 7. Integrated distributions of counterions between the charged planes obtained from molecular dynamics simulation (dashed curve), Poisson–Boltzmann calculation (long-dashed curve) and BD simulation (solid curve).

simulations, Na^+ near the surfaces are hydrated and do not stick directly to the surface, as was the case for Cs^+. These phenomena are obviously not noticeable with BD simulations, nor with Poisson–Boltzmann treatments. However, away from the surfaces, the three distributions are in quite good agreement. Poisson–Boltzmann averages the oscillations, which gives similar integrals for the three curves (see figure 7). These results are very encouraging and show that the Poisson–Boltzmann treatment is a satisfactory starting point for macroscopic descriptions of the system, as soon as the clay is hydrated enough. Moreover, BD simulations will allow us to calculate self-diffusion coefficients of cations in hydrated states, at least when they are not too close to the surfaces of the clay sheets. The calibration of friction coefficients or diffusion coefficients of ions at infinite dilution is a serious problem for BD. The present simulation results were made with values originating from the values in bulk water: they have to be checked and perhaps improved by comparison with other techniques. Further results will follow in a forthcoming paper.

4. Conclusion

In this paper, we have presented multiscale studies of two systems which are examples of charged media in water: in both cases small cations move around large highly negatively charged objects. Several approaches were used at different levels of description: atomic numerical simulations (Monte Carlo and molecular dynamics) at the microscopic one, BD simulations and Poisson–Boltzmann calculations at the mesoscopic ones.

Because of the huge number of particles, microscopic simulations were used to study less hydrated states. These techniques allowed us to obtain structural and dynamical details such as the cation configuration close to the negatively charged surfaces and the method of hydration according to the nature of the counterion. However, the investigation of dynamical

properties of water and counterions around clay surfaces was done for fixed positions of the sheets. The study of dynamical properties of large polyions and their numerous counterions in solution requires the resort to a mesoscopic description. The BD simulation appears to be the appropriate method to describe such systems, where length and timescales are very different.

Our results concerning a relatively hydrated clay showed that microscopic and mesoscopic descriptions are consistent. The dynamics of counterions in the aqueous solution between well separated clay particles may then be simulated from BD simulation.

References

[1] Schmitz K S 1993 *Macroions in Solution and Colloidal Suspension* (New York: VCH)
[2] Israelachvili J N 1992 *Intermolecular and Surface Forces* (London: Academic)
[3] Car R and Parrinello M 1985 *Phys. Rev. Lett.* **55** 2471
[4] Delgado A V (ed) 2002 *Interfacial Electrokinetics and Electrophoresis* (New York: Dekker)
[5] Nägele G 1996 *Phys. Rep.* **272** 215
[6] Hansen J-P and Löwen H 2000 *Annu. Rev. Phys. Chem.* **51** 209
[7] Vlachy V 1999 *Annu. Rev. Phys. Chem.* **50** 145
[8] Oosawa F 1971 *Polyelectrolytes* (New York: Dekker)
[9] Allahyarov E, D'Amico I and Löwen H 1998 *Phys. Rev. Lett.* **81** 1334
[10] Wu J Z, Bratko D, Blanch H W and Prausnitz J M 1999 *J. Chem. Phys.* **111** 7084
[11] Wu J Z, Bratko D, Blanch H W and Prausnitz J M 2000 *Phys. Rev.* E **62** 5273
[12] Jardat M, Cartailler T and Turq P 2001 *J. Chem. Phys.* **115** 1066
[13] Hribar B, Kalyuzhny Yu V and Vlachy V 1996 *Mol. Phys.* **87** 1317
[14] Hribar B and Vlachy V 1997 *J. Phys. Chem.* B **101** 3457
[15] Lobaskin V and Linse P 1998 *J. Chem. Phys.* **109** 3530
[16] Hribar B and Vlachy V 2000 *J. Phys. Chem.* B **104** 4218
[17] Hribar B and Vlachy V 2000 *Biophys. J.* **78** 694
[18] Linse P 1999 *J. Chem. Phys.* **110** 3493
[19] Lobaskin V and Linse P 1999 *J. Chem. Phys.* **111** 4300
[20] Linse P and Lobaskin Vladimir 1999 *Phys. Rev. Lett.* **83** 4208
[21] Linse P and Lobaskin Vladimir 2000 *J. Chem. Phys.* **112**
[22] Jardat M, Bernard O, Turq P and Kneller G R 1999 *J. Chem. Phys.* **110** 7993
[23] de Leeuw S W, Perram J W and Smith E R 1980 *Proc. R. Soc.* A **373** 27
[24] Ermak D L 1975 *J. Chem. Phys.* **62** 4189
[25] Rossky P J, Doll J D and Friedman H L 1978 *J. Chem. Phys.* **69** 4628
[26] Allen M P and Tildesley D J 1987 *Computer Simulation of Liquids* (Oxford: Oxford Science)
[27] Rotne J and Prager S 1969 *J. Chem. Phys.* **50** 4831
[28] Impey R W, Madden P A and McDonald I R 1983 *J. Phys. Chem.* **87** 5071
[29] Zahn K, Méndez-Alcaraz J M and Maret G 1997 *Phys. Rev. Lett.* **79** 175
[30] Nägele G and Baur P 1997 *Physica* A **245** 297
[31] Dufrêche J F, Marry V, Bernard O and Turq P 2001 *Colloids Surf.* A **195** 171
[32] Freund J B 2002 *J. Chem. Phys.* **116** 2194
[33] Delville A and Laszlo P 1989 *New J. Chem.* **13** 481
[34] Dubois M, Zemb T, Belloni L, Delville A, Levitz P and Setton R 1992 *J. Chem. Phys.* **96**
[35] Young D A and Smith D E 2000 *J. Phys. Chem.* B **104** 9163
[36] Boek E S, Coveney P V and Skipper N T 1995 *J. Am. Chem. Soc.* **117** 12 608
[37] Boek E S, Coveney P V and Skipper N T 1995 *Langmuir* **11** 4629
[38] Delville A 1992 *Langmuir* **8** 1796
[39] Chang F-R C, Skipper N T and Sposito G 1998 *Langmuir* **14** 1201
[40] Chang F-R C, Skipper N T and Sposito G 1997 *Langmuir* **13** 2074
[41] Chang F-R C, Skipper N T and Sposito G 1995 *Langmuir* **11** 2734
[42] Skipper N T, Sposito G and Chang F-R C 1995 *Clays Clay Mineral.* **43** 294
[43] Skipper N T, Refson K and McConnell J D C 1991 *J. Chem. Phys.* **94** 7434
[44] Smith D E 1998 *Langmuir* **14** 5959
[45] Sutton R and Sposito G 2001 *J. Colloid Interface Sci.* **237** 174
[46] Marry V, Turq P, Cartailler T and Levesque D 2002 *J. Chem. Phys.* at press

[47] Muurinen A and Lehikoinen J 1995 Nuclear waste commision of finnish power companies *Report* YJT-95-05
[48] Kato H, Muroi M, Yamada N, Ishida H and Sato H 1995 *Scientific Basis for Nuclear Waste Management* vol 18, ed T Murakami and R C Ewing (Pittsburgh, PA: Materials Research Society) p 277
[49] Brindley G W and Brown G 1980 *Crystal Structures of Clays Minerals and their X-Ray Identification* (London: Mineralogical Society)
[50] Maegdefrau E and Hofmann U 1937 *Z. Kristallogr. Kristallgeom. Kristallphys. Kristallchem.* **98** 299
[51] Leote de Carvalho R J F and Skipper N T 2001 *J. Chem. Phys.* **114** 3727
[52] Ochs M, Boonekamp M, Wanner H, Sato H and Yui M 1998 *Radiochim. Acta* **82** 437
[53] Sherwood J D 1992 *Proc. R. Soc.* A **437** 607
[54] Rhee Y-J, Halley J W, Hautman J and Rahman A 1989 *Phys. Rev.* B **40** 36–42
[55] Spohr A 1997 *J. Chem. Phys.* **107** 6342–8